JCI insight

RESEARCH ARTICLE

Pancreatic cancer therapy with combined mesothelin-redirected chimeric antigen receptor T cells and cytokine-armed oncolytic adenoviruses

Keisuke Watanabe,[1] Yanping Luo,[1] Tong Da,[1] Sonia Guedan,[1,2] Marco Ruella,[1,2] John Scholler,[1] Brian Keith,[1,3] Regina M. Young,[1] Boris Engels,[4] Suvi Sorsa,[5,6] Mikko Siurala,[5,6] Riikka Havunen,[5,6] Siri Tähtinen,[5] Akseli Hemminki,[5,6,7] and Carl H. June[1,2,8]

[1]Center for Cellular Immunotherapies, Perelman School of Medicine at the University of Pennsylvania, Philadelphia, Pennsylvania, USA. [2]Parker Institute for Cancer Immunotherapy, University of Pennsylvania, Philadelphia, Pennsylvania, USA. [3]The Wistar Institute, Philadelphia, Pennsylvania, USA. [4]Department of Immuno-Oncology, Novartis Institutes for BioMedical Research, Cambridge, Massachusetts, USA. [5]Cancer Gene Therapy Group, Faculty of Medicine, University of Helsinki, Helsinki, Finland. [6]TILT Biotherapeutics Ltd, Helsinki, Finland. [7]Helsinki University Comprehensive Cancer Center, Helsinki, Finland. [8]Department of Pathology and Laboratory Medicine, Perelman School of Medicine at the University of Pennsylvania, Philadelphia, Pennsylvania, USA.

Pancreatic ductal adenocarcinoma (PDA) is characterized by its highly immunosuppressive tumor microenvironment (TME) that limits T cell infiltration and induces T cell hypofunction. Mesothelin-redirected chimeric antigen receptor T cell (meso-CAR T cell) therapy has shown some efficacy in clinical trials but antitumor efficacy remains modest. We hypothesized that combined meso-CAR T cells with an oncolytic adenovirus expressing TNF-α and IL-2 (Ad5/3-E2F-D24-TNFa-IRES-IL2, or OAd-TNFa-IL2) would improve efficacy. OAd-TNFa-IL2 enhanced the antitumor efficacy of meso-CAR T cells in human-PDA-xenograft immunodeficient mice and efficacy was associated with robustly increased tumor-infiltrating lymphocytes (TILs), enhanced and prolonged T cell function. Mice treated with parental OAd combined with meso-CAR T developed tumor metastasis to the lungs even if primary tumors were controlled. However, no mice treated with combined OAd-TNFa-IL2 and meso-CAR T died of tumor metastasis. We also evaluated this approach in a syngeneic mouse tumor model by combining adenovirus expressing murine TNF-α and IL-2 (Ad-mTNFa-mIL2) and mouse CAR T cells. This approach induced significant tumor regression in mice engrafted with highly aggressive and immunosuppressive PDA tumors. Ad-mTNFa-mIL2 increased both CAR T cell and host T cell infiltration to the tumor and altered host tumor immune status with M1 polarization of macrophages and increased dendritic cell maturation. These findings indicate that combining cytokine-armed oncolytic adenovirus to enhance the efficacy of CAR T cell therapy is a promising approach to overcome the immunosuppressive TME for the treatment of PDA.

Introduction

Chimeric antigen receptor T cell (CAR T cell) therapy has shown significant efficacy in patients with CD19-positive acute lymphoblastic leukemia (1) and lymphoma (2, 3). However, CAR T cell efficacy remains disappointing in the setting of solid tumors (4, 5). There are several factors that can potentially limit the efficacy of CAR T cell therapy in solid tumors and particularly in pancreatic cancer. First, in solid tumors there are no ideal CAR targets like CD19; most tumor-associated antigens are not uniformly expressed in all tumor cells, which can likely lead to tumor escape (6). Moreover, in pancreatic cancer the tumor microenvironment (TME) is particularly immunosuppressive, inhibiting T cell infiltration and functions (7–9). Therefore, developing strategies to address tumor immunosuppression and heterogeneity would represent a vertical advance in the field.

Mesothelin is a promising target for CAR T cell therapy, as it is overexpressed in the majority of pancreatic cancers, mesotheliomas, ovarian cancers, and some lung cancers and it is not expressed on T cells

Conflict of interest: KW, YL, TD, SG, MR, JS, and CHJ work under a research collaboration involving the University of Pennsylvania and the Novartis Institutes for Biomedical Research. KW, SG, MR, JS, and CHJ are inventors on patent application 62/624,707 filed by the University of Pennsylvania and licensed to Novartis. AH is a shareholder in Targovax ASA and TILT Biotherapeutics Ltd.

Submitted: January 2, 2018
Accepted: March 6, 2018
Published: April 5, 2018

Reference information:
JCI Insight. 2018;3(7):e99573. https://doi.org/10.1172/jci.insight.99573.

(10, 11). In previous work by our group, mesothelin-redirected CAR T (meso-CAR T) cells were shown to be effective in mesothelioma xenograft models (12). A phase I clinical trial using T cells engineered to express an anti-mesothelin CAR showed stable disease in 2 out of 6 patients (NCT01897415) (13); however, there is a clear unmet medical need to improve responses in pancreatic ductal adenocarcinoma (PDA) and in patients with other solid tumors.

Oncolytic viruses represent highly promising agents for the treatment of solid tumors, and an oncolytic herpes virus expressing GM-CSF was approved by the US FDA for the therapy of advanced melanoma based on therapeutic benefit demonstrated in a clinical study (14). Oncolytic adenoviruses (OAds) can be programmed to specifically target, replicate in, and kill cancer cells while sparing normal cells. The release of virus progeny results in an exponential increase of the virus inoculum, which can cause direct tumor debulking while providing danger signals necessary to awaken the immune system (15). Importantly, OAds can be genetically modified to express therapeutic transgenes selectively in the TME (16–19). The feasibility and safety of OAds in human patients have been demonstrated in clinical trials (20, 21). Their ability to revert tumor immunosuppression while locally expressing therapeutic transgenes provides a rational strategy for combination with adoptive T cell transfer.

Another possible strategy to modulate the TME in favor of adoptive T cell therapy is the local administration of recombinant cytokines. In this regard, we have previously demonstrated that local tumor delivery of tumor necrosis factor-α (TNF-α) and interleukin-2 (IL-2) can enhance the antitumor efficacy of adoptively transferred OT-I cells (22). These 2 cytokines were selected from a panel of cytokines that are used in clinical oncology in the US and Europe. When combined, TNF-α and IL-2 provide nonoverlapping synergistic effects. TNF-α appears to be responsible for immunological danger signaling and T cell trafficking, while IL-2 activates and propagates T cells locally (16).

Here, we engineered OAd to express TNF-α and IL-2 within the TME and tested this in combination with CAR T cells targeting mesothelin. We hypothesized that OAds expressing cytokines would improve the efficacy of CAR T cell therapy by (a) enhancing and sustaining T cell function and trafficking to the TME, (b) overcoming tumor heterogeneity in antigen expression, and (c) reducing tumor immunosuppression.

Results

Combined OAd-TNFa-IL2 and meso-CAR T cells efficiently lyse target tumor cells. We modified OAds to express TNF-α and IL-2 (OAd-TNFa-IL2) (23) (Supplemental Figure 1A; supplemental material available online with this article; https://doi.org/10.1172/jci.insight.99573DS1). We first tested cytokine production and cell lysis induced by infection of PDA tumor lines. Pancreatic tumor cell lines infected with OAd-TNFa-IL2 secreted large amounts of cytokines and tumor cell lysis was induced in a dose-dependent manner (Supplemental Figure 1, B and C). Incorporation of cytokine transgenes did not enhance the lytic activity of OAds but rather modestly decreased the lytic activity in vitro (Supplemental Figure 1C). This was not surprising, as the additional payload possibly decreases the efficiency of virus replication.

Subsequently, we tested whether OAd-TNFa-IL2 enhances the lytic activity of meso-CAR T cells using real-time cell analysis. Target cell lines BxPC-3, Capan-2, and AsPC-1 expressing various levels of mesothelin were tested; mesothelin was highly positive in Capan-2, medium positive in AsPC-1, but dim in BxPC-3 (Supplemental Figure 1D). BxPC-3 cells expressed very low levels of mesothelin and were resistant to meso-CAR T cells; meso-CAR T cells alone suppressed BxPC-3 cell growth transiently but the cells eventually started growing again. However, when OAd-TNFa-IL2 was combined, meso-CAR T cells efficiently lysed all 3 target tumor cells (Figure 1A). Meso-CAR T cells suppressed Capan-2 tumor cells slowly. The combined OAd-TNFa-IL2 with meso-CAR T cells induced substantially more rapid lysis of Capan-2 cells (Figure 1A). Meso-CAR T cells lysed AsPC-1 cells rapidly and there was no additional benefit of OAd-TNFa-IL2 combination therapy in this in vitro assay (Figure 1A).

OAd-TNFa-IL2 activates T cells and induces T cell proliferation. To test how OAd-TNFa-IL2 enhances the killing activity of meso-CAR T cells, we analyzed T cell proliferation and upregulation of the early T cell activation marker CD69 upon coincubation with OAd-preinfected tumor cell lines. Consistent with the enhanced killing activity (Figure 1A), CD69 upregulation was poorest when stimulated by BxPC-3 cells, while moderate with Capan-2 cells and highest with AsPC-1 cells in the absence of OAd-TNFa-IL2 (Figure 1, B and C). However, OAd-TNFa-IL2 induced enhanced CAR T cell responses, especially when the CAR T cells were stimulated with BxPC-3 cells. Similar to CD69 upregulation, OAd-TNFa-IL2 preinfection significantly

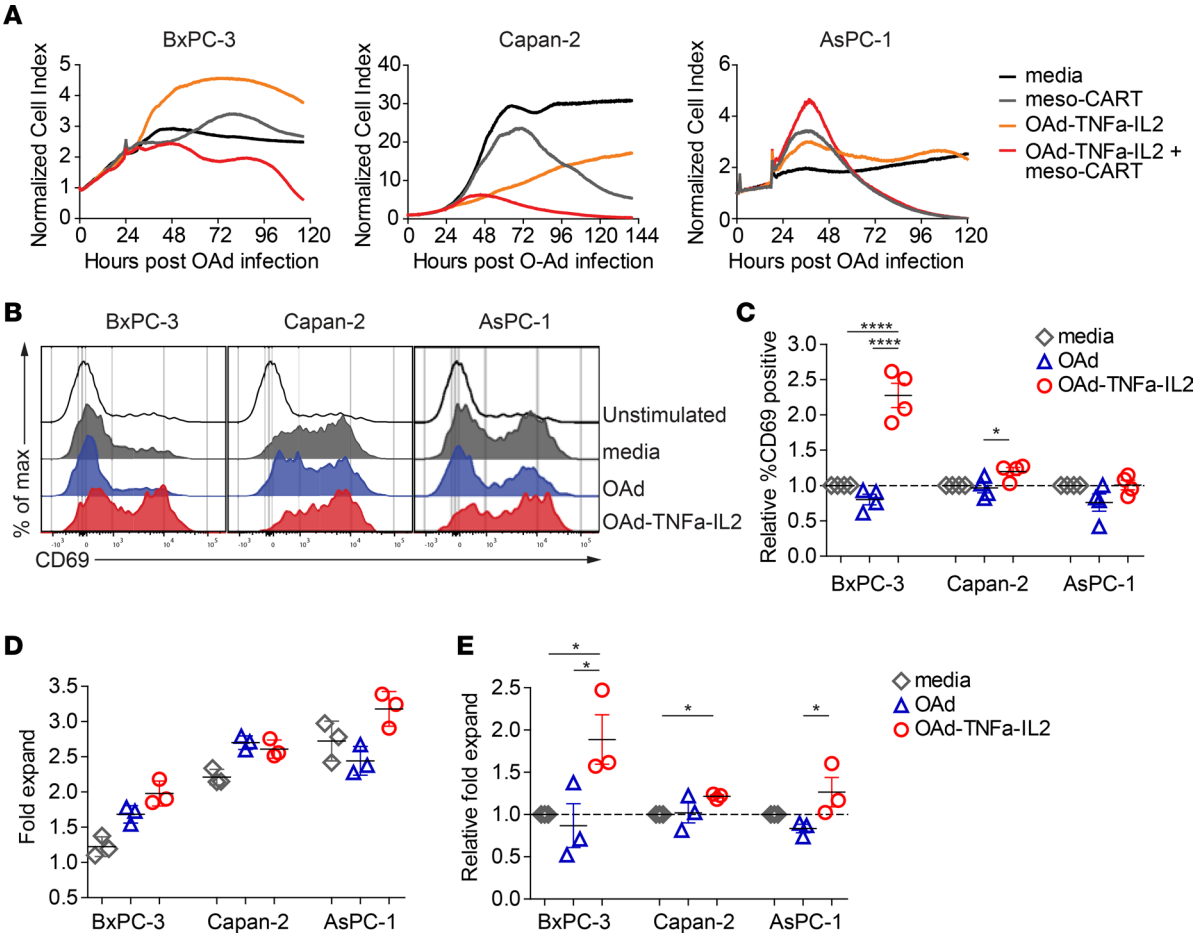

Figure 1. Oncolytic adenovirus (OAd) expressing TNF-α and IL-2, Ad5/3-E2F-D24-TNFa-IRES-IL2 (Ad5/3-OAd-TNFa-IL2), enhances activation, proliferation, and lytic activity of mesothelin-redirected chimeric antigen receptor T cells (meso-CAR T cells). (**A**) Kinetics of pancreatic ductal adenocarcinoma (PDA) tumor cell lysis incubated with the combination of OAd-TNFa-IL2 with meso-CAR T cells measured by the real-time xCELLigence cell analyzer. Means of cell index from triplicate wells are shown. Data are representative of 3 experiments from 3 different donors. (**B**) Upregulation of CD69 on T cells upon stimulation with PDA cell lines preinfected with OAds. Histograms show CD69 expression of T cells at day 3 after coculture with control media alone (unstimulated) or coculture with the indicated tumor cell lines preinfected with either control media (media), parental OAd (OAd), or OAd-TNFa-IL2 (OAd-TNFa-IL2). Data are representative of 3 experiments from 3 different donors. (**C**) Fold increase of percentage CD69-positive T cells from pooled data. Fold increase of percentage CD69-positive T cells by coculturing with tumor cell lines pretreated either with OAd or OAd-TNFa-IL2 relative to those by coculturing with cell lines pretreated with control media (set to 1) are shown. Means and SEM of pooled data from 3 experiments are shown. $*P < 0.05$, $****P < 0.0001$ by 1-way ANOVA with Turkey's post hoc test. (**D**) T cell proliferation upon the stimulation with tumor cell lines preinfected with OAds. Using the same coculture method as in **B** and **C**, T cell expansion was determined at day 5 by flow cytometry using counting beads. Means and SD from triplicate wells are shown. Data are representative of 4 experiments from 3 different donors. (**E**) Relative fold expansion of T cells upon stimulation with tumor cell lines preinfected with OAds. Fold expansion of T cells cocultured with cell lines pretreated with control media was set to 1. Means and SEM of pooled data from 4 experiments are shown. $*P < 0.05$ by 1-way ANOVA with Tukey's post hoc test.

improved CAR T cell proliferation when cultured with the PDA tumor cells (Figure 1, D and E). Thus, OAd-TNFa-IL2 increased target cell killing by meso-CAR T cells presumably by enhancing the function of meso-CAR T cells. Importantly, the most significant enhancement of T cell responses was observed when low-mesothelin-expressing and meso-CAR T cell–resistant BxPC-3 cells were targeted, suggesting that OAd-TNFa-IL2 can be used to augment CAR T cell–mediated killing, particularly when the CAR target antigen expression is limiting.

Combination of OAd-TNFa-IL2 with meso-CAR T cells causes tumor regression in an AsPC-1 tumor xenograft NSG mouse model. To evaluate whether OAd-TNFa-IL2 improves the antitumor efficacy of meso-CAR T cells, we first tested OAd combined with CAR T cell therapy in an AsPC-1 xenograft NOD-SCID-γ-chain$^{-/-}$ (NSG) mouse model (Figure 2A). Meso-CAR T cell monotherapy suppressed tumor growth moderately and OAd-TNFa-IL2 monotherapy failed to suppress tumor growth, although infection was confirmed in tumor immunohistochemistry (IHC) (Supplemental Figure 2). On the other hand, OAd-TNFa-IL2 combined with

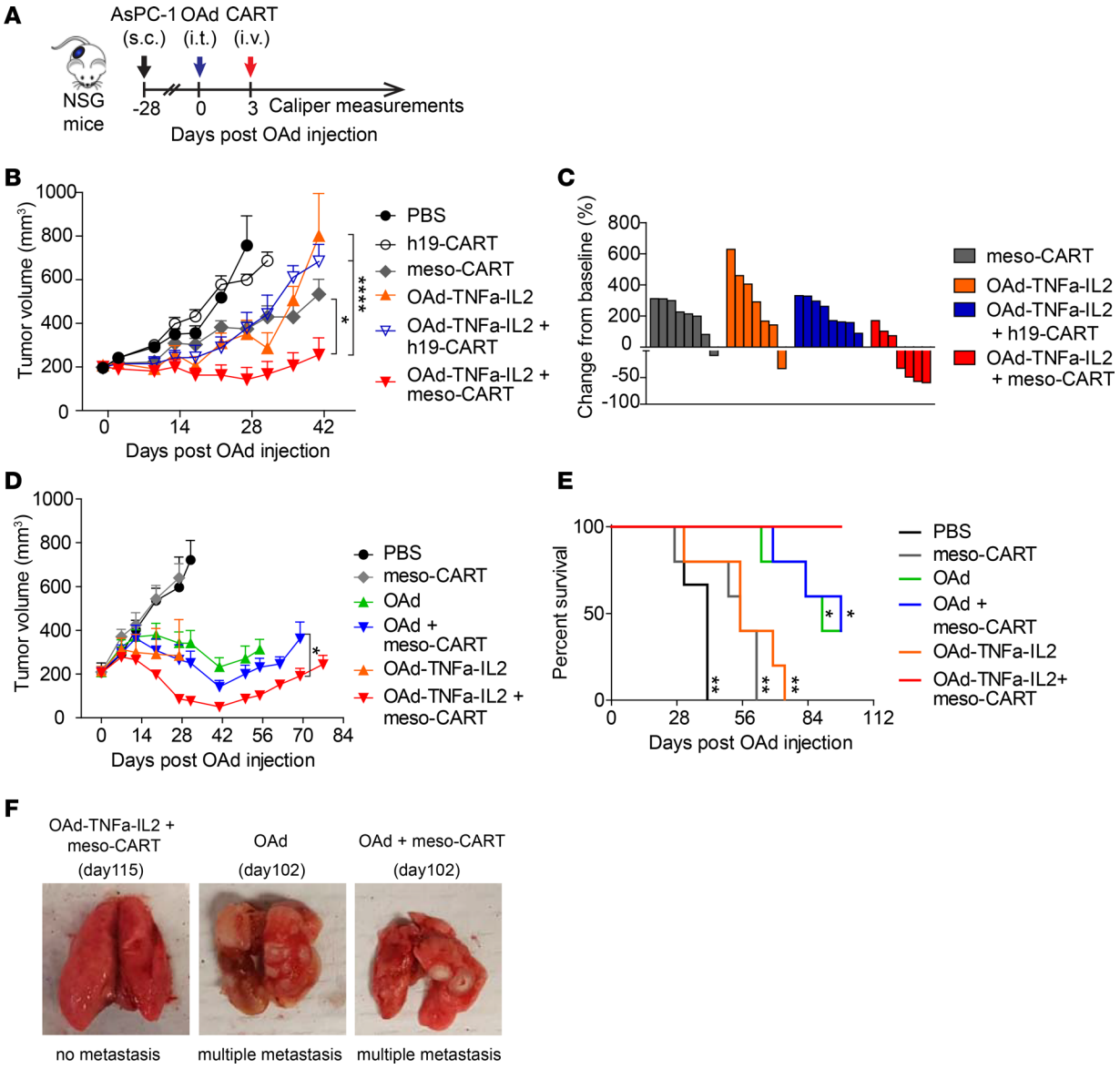

Figure 2. Oncolytic adenovirus (OAd) expressing TNF-α and IL-2, Ad5/3-E2F-D24-TNFa-IRES-IL2 (Ad5/3-OAd-TNFa-IL2), enhances antitumor efficacy of mesothelin-redirected chimeric antigen receptor T cells (meso-CAR T cells) and improves survival in the pancreatic ductal adenocarcinoma (PDA) xenograft model. (**A**) Experimental schematic. AsPC-1 tumor-bearing mice were treated with either intratumoral injection of PBS, 0.95×10^9 virus particles (vp) parental OAd (OAd) or OAd-TNFa-IL2 followed by intravenous injection of either PBS, 1×10^6 meso-CAR T cells or human CD19-redirected CAR T cells (h19-CAR T cells) at day 3 after OAd injection. Tumor volumes were monitored by caliper measurement. (**B**) Tumor volumes by caliper measurement. Data are representative of 2 experiments from 2 different donors. Means and SEM are shown (n = 7 or 8 each). *P < 0.05, ****P < 0.0001 by repeated-measures 2-way ANOVA with Bonferroni's correction. (**C**) Waterfall plots comparing baseline to the endpoint (day 41). Percentage change from baseline to the endpoint is shown. Each bar represents an individual mouse. Data are from the experiment shown in **B**. (**D**) Tumor volumes by caliper measurements. Data are representative of 2 experiments from 2 different donors. Means and SEM are shown (n = 3 each for PBS group and n = 5 each for the other groups). *P < 0.05 by 2-way ANOVA with Bonferroni's correction. (**E**) Kaplan-Meier survival curve. Data are from the experiment shown in **D**. *P < 0.05, **P < 0.01 (vs. OAd-TNFa-IL2 + meso-CAR T cell group) by log-rank test. (**F**) Combined OAd-TNFa-IL2 with meso-CAR T cells can prevent tumor metastasis. Representative lungs from OAd-mTNFa-IL2 + meso-CAR T cell group, OAd group, and OAd + meso-CAR T cell group are shown. The 2 lungs with multiple metastasis shown here are from mice treated with OAd alone or combined OAd and meso-CAR T cells that were euthanized at day 102 due to weight loss (center and right panel). The lung without metastasis is representative from mice treated with combined OAd-TNFa-IL2 and meso-CAR T cells (left panel).

meso-CAR T cells efficiently suppressed tumor growth and achieved a higher rate of tumor regression at the endpoint (Figure 2, B and C). To determine the benefit of cytokine transgenes, we compared the parental OAd and OAd-TNFa-IL2 in combination with meso-CAR T cells in the same mouse model as in Figure 2B. OAd and OAd-TNFa-IL2 monotherapy similarly reduced tumor growth and mice injected with OAd had modestly improved survival compared with OAd-TNFa-IL2 monotherapy (Figure 2, D and E), which may

be because baseline killing activity of parental OAd is higher than that of OAd-TNFa-IL2 (Supplemental Figure 1C). Importantly, the combination of OAd-TNFa-IL2 with meso-CAR T cells clearly induced better tumor regression compared with the combination of parental OAd with meso-CAR T cells. These results suggest that the encoded cytokines have clear benefit to enhance the in vivo antitumor efficacy of CAR T cells, enabling the regression of established PDA tumors that fail to respond to CAR T cell monotherapy. The effect of meso-CAR T cells alone was different between 2 experiments in the same model (Figure 2, B and D), which was possibly because of differential potency of CAR T cells derived from healthy donors. However, OAd-TNFa-IL2 consistently induced meso-CAR T cell efficacy and the combined therapy induced the best tumor suppression (Figure 2, B and D).

Furthermore, mice treated with OAd, OAd-TNFa-IL2, or even the combination of parental OAd and meso-CAR T developed tumor metastasis to the lungs even if primary tumors were controlled (Figure 2F). However, no mice treated with combined OAd-TNFa-IL2 and meso-CAR T died of tumor metastasis. These results suggest that meso-CAR T cells locally activated in the tumor site by OAd-TNFa-IL2 have the potential to target tumors systemically or to prevent PDA cells from egressing from tumors.

OAd-TNFa-IL2 increases tumor-infiltrating T cells. The magnitude of T cell infiltration has a strong impact on the natural history of many types of cancer (24). To determine how parental OAd and OAd-TNFa-IL2 affect tumor-infiltrating lymphocytes (TILs), NSG animals were treated as in Figure 2, and groups of mice were sacrificed at days 14 and 28 for analysis of TILs and tumors. Consistent with the experiment in Figure 2, tumors treated with the combination of OAd-TNFa-IL2 and meso-CAR T cells tended to be smaller in volume on day 28 (Supplemental Figure 3A). In histopathological and flow cytometry (FCM) analysis, tumors treated with the combination of OAd-TNFa-IL2 and meso-CAR T cells were infiltrated with significantly more $CD4^+$ and $CD8^+$ T cells compared with those treated with meso-CAR T cell monotherapy or in combination with the parental OAd (Figure 3, A and B, and Supplemental Figure 3B). The number of $CD8^+$ TILs in IHC was inversely correlated with tumor volume in mice treated with OAd-TNFa-IL2 and meso-CAR T cells but did not correlate in any of the other treatment groups (Figure 3C).

OAd-TNFa-IL2 activates TILs and induces responses of T cells to the tumor. The function of TILs also has a strong impact on the outcome of cancer treatments (24). We analyzed expression of activation markers by TILs at day 28. $CD8^+$ TILs in tumors treated with meso-CAR T cells in combination with OAd-TNFa-IL2 as well as parental OAd expressed higher activation markers CD95 and CD25 compared with meso-CAR T cell monotherapy (Figure 3D), with the same trend in $CD4^+$ TILs (Supplemental Figure 3C), which indicates that OAd and OAd-TNFa-IL2 activated infiltrating CAR T cells.

Subsequently, we analyzed the cytokine profile of bulk tumors for two purposes. The first was to assess whether OAd-TNFa-IL2 successfully delivered cytokine genes to the tumor and made tumor cells produce the corresponding cytokines, and the second was to assess whether T cells in the tumors are functional and responding to the tumors. As a side note, TNF-α and IL-2 are potentially derived either from tumors infected with OAd-TNFa-IL-2, meso-CAR T cells, or both, while human IFN-γ is expected to be produced only by meso-CAR T cells in this mouse model. As expected, TNF-α and IL-2 were detectable from tumors treated with OAd-TNFa-IL2 monotherapy, which indicates vector-mediated secretion of cytokine genes expressed in the PDA tumor cells (Figure 3E). The levels of all cytokines (TNF-α, IL-2, and IFN-γ) were very low or undetectable in tumors treated with meso-CAR T cell monotherapy (Figure 3E), which indicates that T cells in the tumors were hypofunctional and/or that the absolute number of CAR T cells responding to the tumor cells was low. On the other hand, higher levels of all 3 cytokines were detected from tumors treated with the combination of OAd-TNFa-IL2 with meso-CAR T cells than meso-CAR T cell monotherapy (Figure 3E). We also confirmed the same trend in serum, indicating that low but detectable systemic levels of cytokines were produced by this procedure (Supplemental Figure 3D). While it was impossible to separate the relative contribution of CAR T cell–derived IL-2 and TNF-α from OAd-delivered IL-2 and TNF-α, the systemic levels of IFN-γ, which should be derived only from T cells, indicate that the CAR T cell function was enhanced.

Combined OAd-TNFa-IL2 with meso-CAR T cells induces decreased mesothelin intensity, which is associated with antitumor efficacy. Target antigen decrease by adoptive cell therapies is an indicator of an enhanced on-target effect after adoptive transfer with TCR-modified T cells (25). To address how combining OAd-TNFa-IL2 with meso-CAR T cells affects target antigen expression, we quantified mesothelin levels on tumors. Meso-CAR T cells alone or in combination therapy induced decreases in mesothelin intensity within tumors at

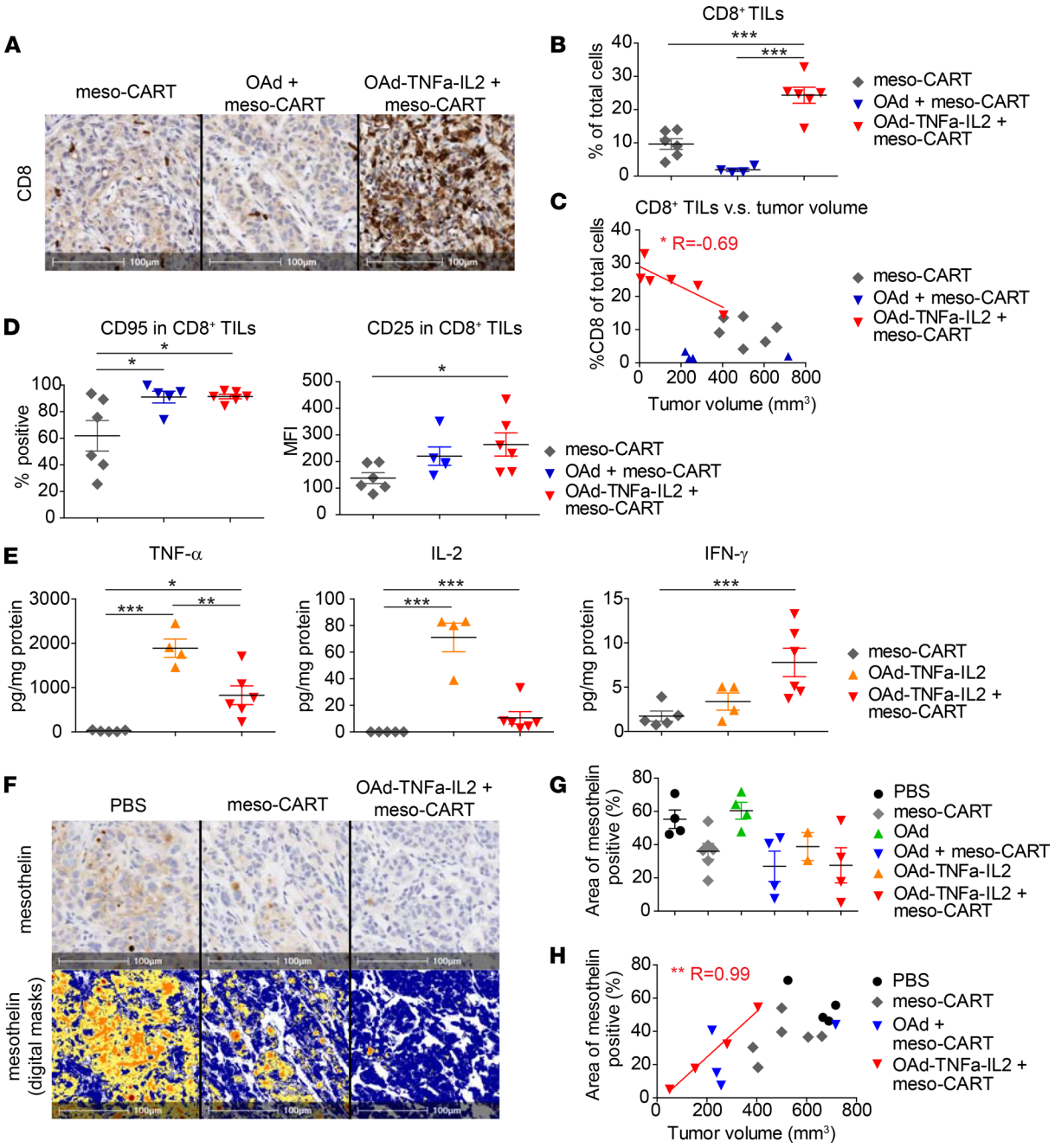

Figure 3. Oncolytic adenovirus (OAd) expressing TNF-α and IL-2, Ad5/3-E2F-D24-TNFa-IRES-IL2 (Ad5/3-OAd-TNFa-IL2), induces robust T cell infiltration of tumors and enhances T cell functions. (**A**) Analysis of CD8+ cell infiltration into the tumor at day 28 by immunohistochemistry (IHC). Representative tumors from the indicated treatment groups are shown. Original magnification, ×20. Scale bars: 100 μm. (**B**) Quantification of tumor-infiltrating lymphocytes (TILs) at day 28. The number of CD8+ TILs was quantified using Aperio ImageScope software. Number of CD8+ cells was normalized as percentage CD8+ cells in total nucleated cells. Data are representative of 2 experiments from 2 different donors. ***$P < 0.001$ by 1-way ANOVA with Tukey's post hoc test. (**C**) Correlation between intensity of CD8+ TILs and tumor volumes. Number of CD8+ T cells (percentage of total cells) quantified from IHC against tumor sizes at day 28 are plotted. A linear regression line is shown. *$P < 0.05$. (**D**) Expression of activation markers on TILs at day 28. T cell activation markers CD95 and CD25 on CD8+ TILs were analyzed by flow cytometry. Data are representative of 2 experiments from 2 different donors. *$P < 0.05$. (**E**) Cytokine profile of the bulk tumors at day 14. Cytokines in the supernatant of the homogenate were analyzed by high-sensitivity LUMINEX assay. *$P < 0.05$, **$P < 0.01$, ***$P < 0.001$ by 1-way ANOVA with Tukey's post hoc test. (**F**) Analysis of mesothelin expression by tumors by IHC at day 28. Mesothelin expression by tumor cells was analyzed by IHC (upper panels). Mesothelin-positive area and staining intensity were analyzed with Aperio ImageScope software. Digital masks over the same fields as upper panels are shown in the lower panels. Blue, negative; Yellow, low intensity; Orange, mid intensity; Red, high intensity. Original magnification, ×20. Scale bars: 100 μm. (**G**) Mesothelin expression by tumors is shown as percentage of mesothelin-positive area. Three tumors (1 from OAd-TNFa-IL2 group and 2 from OAd-TNFa-IL2 + meso-CAR T cell group) are not plotted, as they achieved histological complete remission with no evaluable intact tumor areas. (**H**) Correlation between mesothelin expression and tumor sizes. Areas of mesothelin positivity (%) are plotted against tumor size at day 28. Linear regression lines are shown. *$P < 0.05$, **$P < 0.01$. For vertical scatter plots, bars represent mean and SEM. $n = 4$–6 each (**B**–**E**, and **G**).

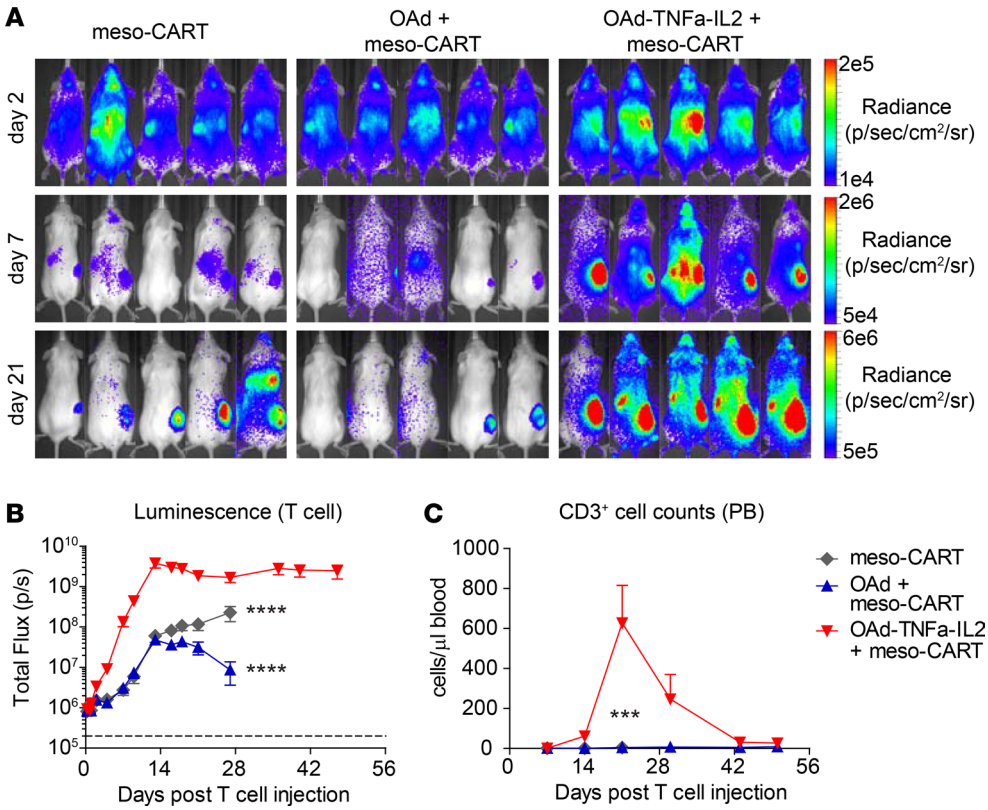

Figure 4. Oncolytic adenovirus (OAd) expressing TNF-α and IL-2, Ad5/3-E2F-D24-TNFa-IRES-IL2 (Ad5/3-OAd-TNFa-IL2), induces robust and persistent mesothelin-redirected chimeric antigen receptor T cell (meso-CAR T cell) accumulation in the tumor and improves T cell engraftment. (**A** and **B**) Trafficking of meso-CAR T cells by bioluminescence imaging (BLI). Using the same treatment schedule as in Figure 2A, luciferase-expressing meso-CAR T cells (CBR-meso-CAR T cells) were tracked by BLI. Luminescence from tumor areas was analyzed (**B**). Means and SEM are shown (n = 5 each). ****P < 0.0001 (vs. OAd-TNFa-IL2 + meso-CAR T cell group at any time points between day 13 and day 28) by 2-way repeated-measures ANOVA with Bonferroni's correction. (**C**) CD3⁺ T cell counts in peripheral blood (PB). T cell number was determined by Trucount analysis. Means and SEM are shown (n = 5 each). ***P < 0.001 (vs. OAd-TNFa-IL2 + meso-CAR T cell group) by repeated-measures 2-way ANOVA.

day 28, which is consistent with selection for tumor cell variants expressing lower levels of mesothelin (Figure 3, F and G). Meso-CAR T cells induced the most significant decrease in mesothelin expression when combined with OAd-TNFa-IL2, and the mesothelin decrease correlated with antitumor efficacy (Figure 3H). These results suggest that OAd-TNFa-IL2 enhanced on-target lytic activity of meso-CAR T cells, which is associated with improved tumor regression.

OAd-TNFa-IL2 induces robust and sustained meso-CAR T cell accumulation in tumors. As FCM and histological analysis at days 14 and 28 indicated that OAd-TNFa-IL2 increases CAR T cell recruitment (Figure 3, A and B, and Supplemental Figure 3B), we performed T cell trafficking assays to determine the precise kinetics of meso-CAR T cell distribution. As early as day 2 after the injection, meso-CAR T cells in combination with OAd-TNFa-IL2 started to show higher accumulation at the tumor site and reached a 2-log higher accumulation compared with parental OAd at day 13 (Figure 4, A and B). OAd-TNFa-IL2 also enhanced T cell engraftment in peripheral blood, with the peak at day 21 (Figure 4C). Interestingly, meso-CAR T cell expansion was transient in peripheral blood (Figure 4C), while meso-CAR T cells persisted at the tumor site with sustained high-level accumulation for at least 50 days (Figure 4, A and B). These results indicate that the enhanced proliferation of CAR T cells by OAd-TNFa-IL-2 is due to recognition of tumor-associated mesothelin rather than xenogeneic antigens and graft-versus-host disease.

T cell factors dominate the causes of tumor resistance rather than target antigen loss in meso-CAR T therapies. Target antigen loss and T cell hypofunction or insufficient tumor infiltration are major causes of tumor relapse for adoptive cell therapies (6). To explore the causes of tumor resistance, we analyzed tumors and TILs late after treatment. We sacrificed the mice treated with meso-CAR T cell monotherapy and mice treated with combined OAd-TNFa-IL2 and meso-CAR T cells on day 57 in the experiment shown in Figure 2, B and C. Five out of 7 mice from the meso-CAR T cell group and all 7 mice in the OAd-TNFa-IL2 plus meso-CAR

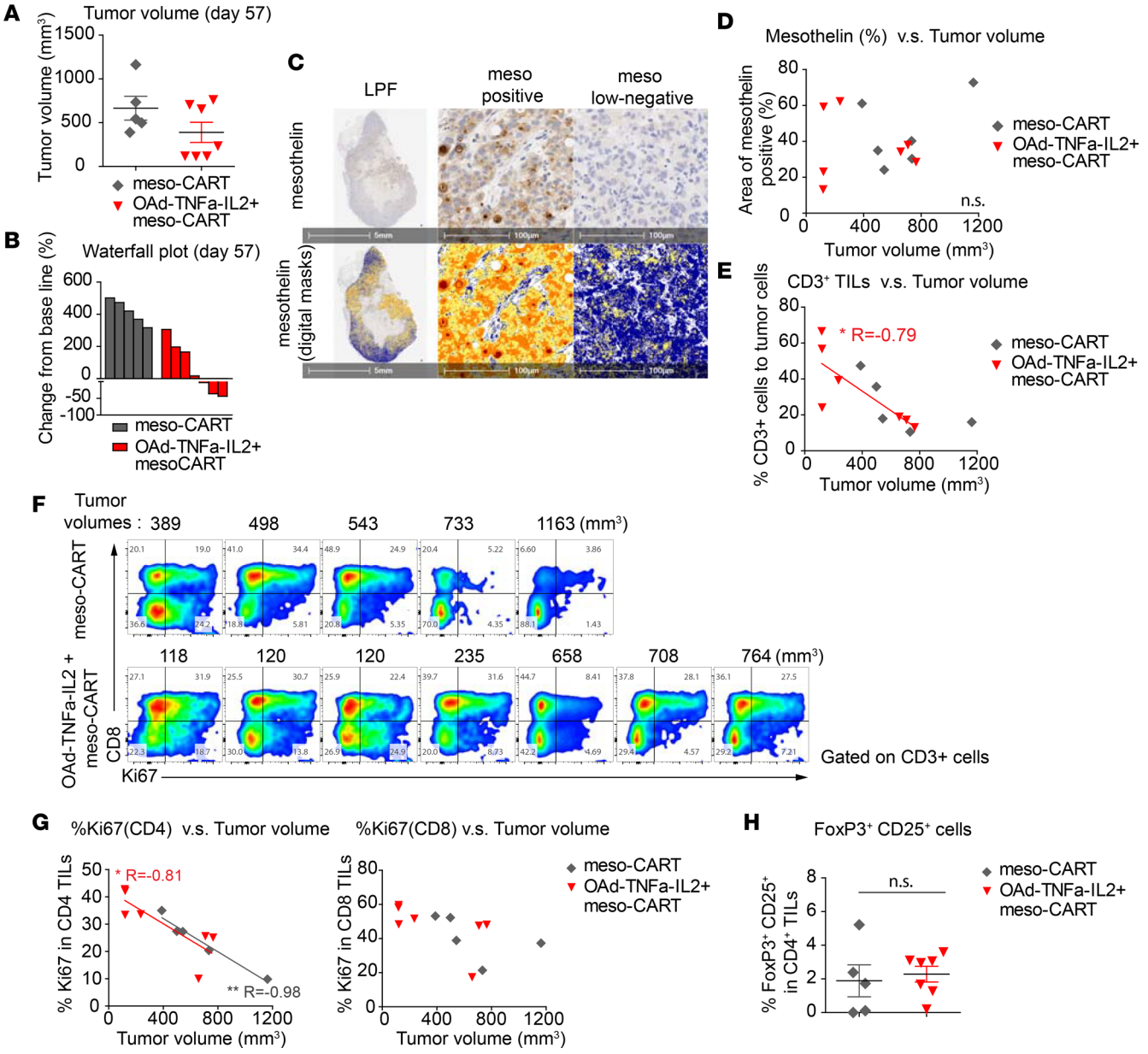

Figure 5. Intensity of functional T cell infiltration is associated with sustained tumor regression after mesothelin-redirected chimeric antigen receptor T cells (meso-CAR T cells) and oncolytic adenovirus expressing TNF-α and IL-2, Ad5/3-E2F-D24-TNFa-IRES-IL2 (Ad5/3-OAd-TNFa-IL2) treatment in an AsPC-1 tumor xenograft immunodeficient mouse model. (**A** and **B**) Tumor volumes by caliper measurements and waterfall plots comparing baseline to day 57. Mice from the indicated 2 treatment groups were observed until day 57 and then sacrificed. Data for the surviving mice (6 of 8 mice for meso-CAR T cell group and all 7 mice for OAd-TNFa-IL2 + meso-CAR T cell group) is shown. Bars represent means and SEM in **A**. (**C**) Mesothelin expression on tumors at day 57. Mesothelin expression of the representative tumor from OAd-TNFa-IL2 + meso-CAR T cell group by immunohistochemistry (IHC) (upper panels) and digital masks (lower panels) on the same fields as upper panels are shown. The low-power fields (LPFs) show central necrosis and heterogeneity in mesothelin intensity (left panels). Representative high-power fields (HPFs) of mesothelin-positive area (center panels) and mesothelin low-negative area (right panels) from the tumor shown in the LPF. Blue, negative; Yellow, low intensity; Orange, mid intensity; Red, high intensity. Original magnification, ×20. Scale bars: 5 mm for LPF, 100 μm for HPF. (**D**) Correlation between mesothelin expression and tumor size at day 57. Areas of mesothelin positivity (%) against tumor volumes are plotted. n.s., not significant. (**E**) Correlation between CD3⁺ tumor-infiltrating lymphocyte (TIL) density and tumor volumes. Percentage CD3⁺ cells to tumor cells against tumor volumes are plotted. A linear regression line is shown. *$P < 0.05$. (**F**) Expression of Ki67 by TILs. Ki67 expression by CD3⁺ TILs from surviving mice was analyzed by flow cytometry (FCM). Columns are arranged in the order of tumor volumes at day 57 and the tumor sizes are shown at the top of each column. (**G**) Correlation between Ki67 expression by CD4⁺ and CD8⁺ TILs and tumor volumes. Percentage Ki67 expression by CD4⁺ TILs or CD8⁺ TILs against tumor volumes are plotted. Linear regression lines are shown. *$P < 0.05$, **$P < 0.01$. (**H**) Analysis of Treg infiltration into the tumor. CD25⁺FoxP3⁺ Tregs in CD4⁺ TILs were analyzed by FCM. Bars represent means and SEM. n.s., not significant by Student's *t* test.

T cell group were surviving at day 57. Four tumors from the OAd-TNFa-IL2 plus meso-CAR T cell group had sustained regression, while 3 other tumors showed regrowth (Figure 5, A and B). The tumors retained mesothelin expression, but the distribution was heterogeneous with areas of negative or low expression (Figure 5C). However, the residual mesothelin intensity did not correlate with tumor regression on day 57 (Figure 5D), unlike on day 28 (Figure 3H). On the other hand, the density of $CD3^+$ TILs still clearly correlated with antitumor efficacy at this later time point (Figure 5E). By FCM, both $CD4^+$ and $CD8^+$ CAR T cells were recovered from the tumors (Figure 5F). The fraction of $CD4^+$ TILs expressing Ki67 was inversely correlated with tumor volume (Figure 5G). We also confirmed that the percentage of $CD25^+FoxP3^+$ Tregs in $CD4^+$ TILs was low and there was no significant difference between the meso-CAR T cell monotherapy group and the combination of OAd-TNFa-IL2 plus meso-CAR T cell group (Figure 5H). These results indicate that loss of mesothelin expression and CAR T cell hypofunction may both contribute to tumor recurrence, and it is likely that loss of function or induction of exhaustion may be a major factor explaining delayed tumor progression in this model.

Syngeneic immunocompetent mouse PDA model to test combination therapy with CAR T cells and adenovirus expressing cytokines. Human xenograft NSG mouse models are useful tools to define the antitumor efficacy of new treatments. However, they lack a functional immune system and do not faithfully reproduce the human TME (26), which prevents evaluation of mechanisms of OAd therapy other than direct enhancement of CAR T cells. Therefore, we established engineered mouse T cells expressing an anti–mouse mesothelin CAR with murine 4-1BB and murine CD3-ζ signaling domains (mmeso-CAR T) (Supplemental Figure 4, A and B). In vitro, the mmeso-CAR T cells effectively lysed PDA7940b cells derived from the genetically engineered $Kras^{LSL.G12D/+}p53^{R172H/+}$ mouse model, while control h19-CAR T cells did not (Supplemental Figure 4C).

Established mouse pancreatic tumors are resistant to mmeso-CAR T cells, but combining Ad-mTNFa-mIL2 enables tumor regression. We tested the antitumor efficacy of mmeso-CAR T cells in combination with an adenovirus expressing murine TNF-α and murine IL-2 in immunocompetent mice engrafted with syngeneic PDA7940b tumor (Figure 6A). We used nonreplicative serotype 5 adenovirus coding for murine TNF-α (Ad-mTNFa) and murine IL-2 (Ad-mIL2) with CMV promoters to deliver cytokine genes to mouse tumors, recognizing that murine cells are nonpermissive for human adenoviral replication (16). These viruses could infect PDA7940 cells and induce cytokine production in a dose-dependent manner in vitro (Supplemental Figure 4D). Established PDA7940b tumors were highly aggressive and even multiple weekly dosing of mmeso-CAR T cell infusions failed to suppress tumor growth. In contrast, combined Ad-mTNFa-mIL2 (1:1 ratio mixture of Ad-mTNFa and Ad-mIL2) with mmeso-CAR T cells had robust antitumor efficacy even though control Ad-luc did not significantly enhance the antitumor efficacy of mmeso-CAR T cells (Figure 6B). Interestingly, Ad-mTNFa-mIL2 monotherapy or in combination with control h19-CAR T cells also showed partial antitumor efficacy, highlighting the importance of therapeutic transgenes in an immunocompetent setting, which likely activate endogenous adaptive and innate antitumor activity.

Ad-mTNFa-mIL2 recruits both adoptively transferred meso-CAR T cells and host T cells to PDA tumors. It has been reported that mouse PDA tumors are "cold tumors" with low-level T cell infiltration that is associated with poor responses to immunotherapies (27). To determine whether Ad-mTNFa-mIL2 could improve T cell infiltration into the tumor bed, we first tracked CAR T cells after the first injection by bioluminescence imaging (BLI) using click beetle red luciferase–expressing (CBR-expressing) CAR T cells. Meso-CAR T cells alone showed transient low-level engraftment. In contrast, Ad-mTNFa-mIL2 induced robustly higher meso-CAR T cell accumulation that peaked on day 6 after injection (Figure 6C). Ad-mTNFa-mIL2 also induced low-level h19-CAR T cell accumulation, although h19-CAR T cells alone did not accumulate in the tumor (Figure 6C). We also analyzed TILs at day 12 by FCM using the same experimental schedule (Figure 6A). Tumors were poorly infiltrated with adoptively transferred T cells and host T cells after mmeso-CAR T cell monotherapy. In contrast, Ad-mTNFa-mIL2 induced significantly higher donor and host $CD4^+$ and $CD8^+$ T cell infiltration in the tumor (Figure 6D).

Ad-mTNFa-mIL2 alters host immune status and induces M1 polarization of macrophages and DC maturation. It has been reported that KPC tumors faithfully reproduce the highly immunosuppressive phenotype of human PDA (27). The above results suggest that mIL-2 and mTNF-α delivered by adenoviruses enhanced the antitumor effect of adoptively transferred mmeso-CAR T cells that may be additionally augmented by CAR-independent host immunity. M1 macrophages are critical components involved in innate antitumor immunity (28). To assess how Ad-mTNFa-mIL2 alters host immune suppression we analyzed the phenotypes of macrophages

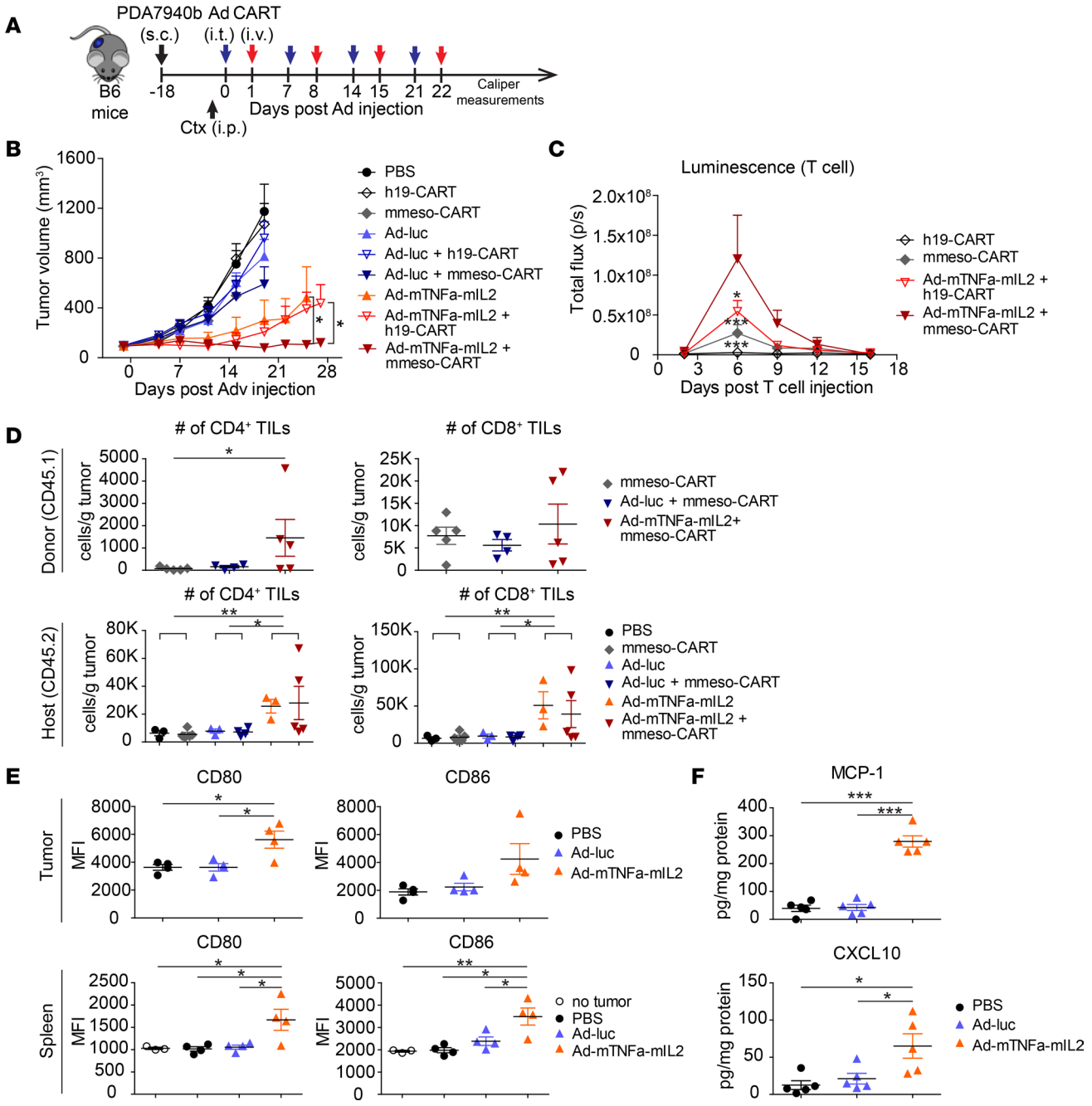

Figure 6. Combined mouse TNF-α and IL-2 delivered by adenoviruses with mouse mesothelin-redirected chimeric antigen receptor T cells (mmeso-CAR T cells) enables significant tumor suppression by enhancing both CAR-dependent and CAR-independent host immunity in a syngeneic pancreatic ductal adenocarcinoma–engrafted immunocompetent mouse model. (**A**) Experimental schematic. Established PDA7940b tumors were treated either with intratumoral injection of PBS, 1×10^9 virus particles (vp) of control adenovirus (Ad-luc), or 1:1 mixture of Ad-mTNFa and Ad-mIL2 (total 1×10^9 vp) (Ad-mTNFa-mIL2) followed by intravenous injection of either PBS, 5×10^6 mmeso-CAR T cells or human-CD19-redirected chimeric antigen receptor T cells (h19-CAR T cells) at day 1 after Ad injection. Mice were preconditioned with intraperitoneal injection of 120 mg/kg cyclophosphamide (Ctx) at 24 hours before the first T cell injection. Adenovirus and CAR T cell injections were repeated 4 times weekly. (**B**) Tumor volumes by caliper measurements. Means and SEM are shown (n = 5 or 6 each). Representative of 2 experiments. *$P < 0.05$ by repeated-measures 2-way ANOVA. (**C**) Trafficking of CAR T cells by bioluminescence imaging (BLI). Luciferase-expressing CAR T cells (CBR-CAR T cells) after the first single injection were tracked by BLI. Experiment was performed with the same schedule as in **A**, but T cell injection was performed just once. Luminescence from tumor area was analyzed. Means and SEM are shown (n = 5 each). *$P <$ 0.05, ***$P < 0.001$ (vs. Ad-mTNFa-mIL2 + mmeso-CAR T cell group) by repeated-measures 2-way ANOVA with Bonferroni's correction. (**D**) Recruitment of donor-derived tumor-infiltrating lymphocytes (TILs) and host TILs at day 12. Number of CD4+ and CD8+ TILs were analyzed by flow cytometry (FCM). Origin of T cells was determined by staining of CD45.1 (donor) and CD45.2 (host). K, ×1,000 (y-axis label). *$P < 0.05$, **$P < 0.01$ by 1-way ANOVA with Tukey's post hoc test. (**E**) Phenotype of macrophages at day 1. CD80 and CD86 expression on tumor-infiltrating macrophages and spleen macrophages was analyzed at 24 hours after intratumoral injection of either PBS, Ad-luc, or Ad-mTNFa-mIL2 by FCM. *$P < 0.05$, **$P < 0.01$ by 1-way ANOVA with Tukey's post hoc test. (**F**) Chemokine analysis of bulk tumors at day 1. Chemokines from bulk tumor homogenate at day 1 after adenovirus injection were analyzed by LUMINEX assay. *$P < 0.05$, ***$P < 0.001$ by 1-way ANOVA with Tukey's post hoc test. For vertical scatter plots in **D**–**F**, bars represent means and SEM (n = 3–5 each).

and dendritic cells (DCs). Ad-mTNFa-mIL2 clearly induced upregulation of CD80 and CD86 expression from F4/80$^+$ macrophages both in tumors and spleens on day 1 after intratumoral injection (Figure 6E), which is consistent with M1 polarization. In contrast, injection of control Ad-luc did not induce upregulation of CD80 and CD86. Moreover, Ad-mTNFa-mIL2 also induced CD11c$^+$ DC maturation assessed by CD80 and CD86 upregulation both in tumors and spleens (Supplemental Figure 4E).

Ad-mTNFa-mIL2 creates a chemokine-rich TME, which can attract immune cells. Chemokines are secondary proinflammatory mediators that are induced by primary proinflammatory mediators such as interleukins or tumor necrosis factors and have critical roles for recruitment of immune cells (29). We investigated the alteration of chemokine expression in tumors at day 1 after adenovirus injection. Ad-mTNFa-mIL2 but not Ad-luc clearly increased chemokines that can attract immune cells: monocyte chemoattractant protein-1 (MCP-1), C-X-C motif chemokine ligand 10 (CXCL-10), and RANTES (Figure 6F and Supplemental Figure 4F), which are reported as TNF-α–inducible chemokines and function to attract immune cells including T cells, NK cells, macrophages, and DCs (30–32). These results suggest that in addition to direct efficacy of mTNF-α and mIL-2 delivered by adenoviruses, secondarily induced chemokines also contribute to recruiting adoptively transferred CAR T cells and host immune cells to the tumors.

Taken together, these results suggest that Ad-mTNFa-mIL2 has the potential to enhance the efficacy of mmeso-CAR T cell therapy by altering the host immune status to a more proinflammatory antitumor state and by inducing both CAR-dependent and CAR-independent immune reactions against pancreatic cancer.

Discussion

The central issues for adoptive cell therapies against solid tumors are poor T cell infiltration, hypofunction of T cells in the tumors, and tumor heterogeneity (4–6). PDA is characterized by a strongly immunosuppressive TME, which can limit the efficacy of adoptively transferred T cells (7–9). The goals of the present study were to establish effective therapy against PDA by combining 2 promising immunotherapeutic approaches, OAd expressing cytokines and CAR T cells and to reveal the mechanisms of synergy and resistance to this combination therapy for PDA in syngeneic and xenogeneic experiments. Our work confirms and extends work by Nishio and colleagues, who found that a different OAd armed with RANTES and IL-15 augmented apoptosis in tumor cells exposed to CAR T cells, while the intratumoral release of both RANTES and IL-15 attracted CAR T cells and promoted their local survival, respectively, and increased the overall survival of neuroblastoma-bearing mice (17).

It has been reported that PDA typically has few TILs, whereas the lymphocytic populations are predominantly found in the stroma surrounding the tumor mass (33), and recent studies suggest that the T cells in long-term survivors with pancreatic cancer target neoantigens (34). The presence of high numbers of TILs and extensive infiltration are major indicators of favorable patient prognosis and positive therapeutic responses in treating several solid tumors, including colorectal cancer (35), lung cancer (36), and ovarian carcinomas (37, 38). Although it is not yet clear whether the intensity of CAR TILs directly correlates with their efficacy or patient outcome in solid tumors, it is reasonable to assume that augmentation of CAR TILs will enhance antitumor efficacy. We demonstrated that OAd-TNFa-IL2 induced robust CAR T cell infiltration, which was clearly associated with enhanced antitumor efficacy. TNF-α is reported to induce T cell–attractive chemokines (39) and IL-2 itself has ability to induce proliferation and chemotaxis of T cells (40). Moreover, in the context of local delivery with adenovirus, TNF-α appears to mediate activation of innate immunity and attraction of T cells to the tumors potentially through chemokine induction, which is further enhanced by addition of IL-2 (16). Taken together, the main mechanism of enhanced antitumor efficacy by the combination cytokine-armed OAd plus CAR T cell therapy was associated with robustly enhanced and sustained T cell function and persistence in the tumor.

We further investigated the mechanisms of the combination therapy by focusing on target antigen expression. O'Rourke et al. reported from the first-in-human study of epidermal growth factor receptor variant III–redirected (EGFRvIII-redirected) CAR T cell therapy against glioblastoma (GBM) that most of patients had specific loss or decrease of EGFRvIII target antigen expression in tumors resected after CAR T cell infusion (6). This finding supports the idea that additional therapies to enhance epitope spreading such as our approach to combine OAds with CAR T cells may be needed to prevent antigen escape. We found that mesothelin intensity in the TME was a predictor of response early after the combined OAd-TNFa-IL2 and meso-CAR T cell treatment but not after meso-CAR T cell monotherapy, which indicated

that OAd-TNFa-IL2 induced sufficient on-target efficacy of meso-CAR T cells to lyse mesothelin-positive tumor cells. A unique advantage of the combined OAd and CAR T cell therapy is that OAds recognize and infect tumor cells using different antigens from the ones that CAR T cells typically recognize. The chimeric serotype 5/3 OAds that we used recognize desmoglein-2 (DSG-2) as a target (41), whereas CAR T cells recognize mesothelin as a target. It is likely that OAds can target and suppress mesothelin-low or -negative tumor cells. Indeed, mesothelin intensity no longer correlated with tumor suppression at the time of tumor progression, whereas T cell factors such as the intensity of T cell infiltration and enhanced T cell function was an important factor, suggesting that direct lysis of tumor cells by OAds, which can occur independently of mesothelin, is another important factor for tumor suppression in addition to the enhanced on-target effects of meso-CAR T cells. A potential weakness of our strategy using vector-encoded IL-2 is activation and/or induction of Tregs in the TME. Although we did not observe increased Treg infiltration to the tumors treated with combined OAd-TNFa-IL2 and meso-CAR T cells in our human-PDA-xenograft mouse model, this could be explained by the use of immunocompromised mice. Indeed, our previous study with murine IL-2 and OT-I T cells in the ovalbumin-expressing B16 melanoma (B16.OVA) immunocompetent mouse model has revealed that simultaneous antitumor and immunosuppressive pathways (Tregs) appear to be induced with IL-2 (42). However, even with evidence of the dual effect of IL-2, adenovirus-delivered murine TNF-α and IL-2 successfully enhanced the antitumor efficacy of adoptively transferred OT-1 T cells (16). Our previous reports combined with the present observations suggest that locally delivered high concentration IL-2 by adenoviruses may induce antitumor effects while dominating the potential weakness of the IL-2 construct, Treg induction. From these observations, meso-CAR T cells and OAd-TNFa-IL2 are an attractive combination to improve the treatment of PDA by overcoming T cell hypofunction and tumor heterogeneity in target antigen expression.

We investigated whether OAd-TNFa-IL2 could enhance the efficacy of meso-CAR T cells in an AsPC-1 tumor xenograft NSG mouse model. Even though parental OAd combined with meso-CAR T cells or parental OAd monotherapy could suppress primary tumors to some extent, these mice typically died of tumor metastasis even in cases where primary tumors were being controlled. On the other hand, mice treated with combined OAd-TNFa-IL2 and meso-CAR T cells did not develop tumor metastasis. These results suggest that locally activated meso-CAR T cells at the primary tumor site exerted systemic immunosurveillance to prevent tumor progression. This is an important aspect of this combination therapy, as patients frequently die from tumor metastasis in PDA (43).

Regarding the immunocompetent model, although replication-deficient adenoviruses do not directly lyse infected tumor cells, Ad-mTNFa-mIL2 rapidly and aggressively reduced tumor growth after virus injection. These results indicate that host innate immunity such as macrophages, DCs, and NK cells contributed to tumor control. We observed Ad-mTNFa-mIL2–induced infiltration of non-CAR host T cells in addition to adoptively transferred donor CAR T cells. Ad-mTNFa-mIL2 modulated the tumor immunosuppression by promoting M1 polarization of macrophages and maturation of DCs. As we previously found that OAd therapy can prime T cells that recognize additional tumor antigens via T cell receptors (TCR-T cells) in the ovalbumin-expressing B16 melanoma mouse model (44), this reprogramming of the TME is expected to prime TCR-T cells that recognize tumor neoantigens by epitope spreading. Thus, our immunocompetent mouse model revealed that adenovirus could enhance the efficacy of CAR T cell therapy not only by directly enhancing CAR T cell functions but also by inducing CAR-independent immunity of host cells, perhaps by eliciting neoantigen responses to overcome tumor heterogeneity and tumor escape caused by target antigen loss.

One limitation of our study is that we used established PDA tumor lines and we have not yet tested primary PDA tumor xenografts. In addition, NSG mice do not have a complete immune system and human xenograft models do not reproduce the human TME (26). Recent studies indicated that the main impact of oncolytic polio and herpes virus therapy is its immune-modulating effects (45, 46). The lack of an intact immune system in NSG mice may overlook these important immunological aspects of OAd therapy. Therefore, we tested this combination therapy in a fully immunocompetent setting. Our newly established mouse mesothelin-redirected CAR T cells enabled testing the mmeso-CAR T cell therapies in a fully immunocompetent setting. To our knowledge, this is the first report demonstrating that mouse CAR T cells targeting native syngeneic mouse tumor antigens in solid tumors augment the antitumor efficacy of adenoviral delivery of cytokine transgenes. Even in the highly immunosuppressive PDA TME, Ad-mTNFa-mIL2 successfully enhanced the antitumor efficacy with mmeso-CAR T cells.

In summary, we describe a potentially novel combination therapy of oncolytic adenovirus expressing TNF-α and IL-2 with meso-CAR T cells in the treatment of PDA. Meso-CAR T cells failed to work effectively in PDA tumors as monotherapy, but combining it with OAds expressing TNF-α and IL-2 enabled effective meso-CAR T cell therapy by modulating the immunosuppressive TME and inducing CAR-dependent and CAR-independent host immunities. In addition to our preclinical data reported here, the safety profiles of the same platform of OAds used in our experiments have already been evaluated as monotherapies in several clinical trials (20, 21), and provide a compelling rationale for CAR T cell plus OAd combination therapy targeting PDA.

Methods

Generation of human meso-CAR T cells. Anti-mesothelin CAR containing the CD3-ζ signaling domain and the 4-1BB costimulatory domain was generated as previously described (12). T cells from normal donors were transduced with lentivirus to express anti-mesothelin CAR.

Generation of mmeso-CAR T cells. A human B cell–derived scFv library was screened using phage display technology (47) in order to obtain mouse mesothelin–binding scFvs to be incorporated into CAR constructs. mmeso-CAR was constructed by fusing anti-mesothelin scFv to a mouse CD3-ζ signaling domain and a mouse 4-1BB costimulatory domain. The CAR was subcloned into the MSGV vector and packaged in the Plat E cell line to obtain the retrovirus. For the T cell transduction, spleens were harvested from CD45.1 donor mice and T cells were purified with mouse T cell isolation beads (Stemcell Technologies). Purified mouse T cells were activated with anti-mouse CD3 and CD28 antibody–coated beads (Dynabeads, Thermo Fisher Scientific) at a bead/cell ratio of 2:1 and then transduced with retroviral vector MSGV for CAR expression on recombinant human fibronectin–coated (Retronectin, Takara Bio USA) plates at day 3 after bead stimulation. Recombinant mouse IL-2 (50 U/ml) was supplemented at day 1 and then supplemented with fresh media containing 50 U/ml IL-2 every day. Mouse CAR T cells were harvested and subjected to the in vivo experiments at day 5.

Cell lines. BxPC-3, Capan-2, and AsPC-1 cell lines were obtained from the American Type Culture Collection (ATCC) and authenticated by the University of Arizona Genetics Core. The PDA7940b cell line, which was established from the $Kras^{LSL.G12D/+}p53^{R172H/+}$ (KPC) mouse pancreatic tumor model (27), was provided by Gregory Beatty (University of Pennsylvania). All cell lines were tested for the presence of mycoplasma contamination (MycoAlert Mycoplasma Detection Kit, Lonza). BxPC-3 and AsPC-1 were maintained in culture with DMEM/F12 (1:1) (Gibco, Life Technologies) supplemented with 20% FBS (Seradigm) and 50 IU/ml penicillin/streptomycin (Gibco, Life Technologies). Capan-2 and PDA7940b were maintained in culture with DMEM (Gibco, Life Technologies) supplemented with 10% FBS and 50 IU/ml penicillin/streptomycin.

Adenovirus construction. The oncolytic adenovirus that has a 24-base-pair deletion in constant region 2 of the E1A gene and chimeric serotype 5 shaft and serotype 3 knob (Ad5/3-D24) (OAd) was constructed and produced as described previously (48). Parental OAd was modified by adding a tumor-specific E2F1 promoter driving an E1 gene deleted at the retinoblastoma protein binding site (Δ24) and further modified by encoding TNF-α and IL-2 genes to deliver cytokine genes to target tumor cells (Ad5/3-E2F-D24-TNFa-IRES-IL2, or OAd-TNFa-IL2 for short) (23) (Supplemental Figure 1A). Replication-incompetent adenovirus serotype 5 expressing luciferase (Ad-luc) and adenovirus serotype 5 expressing murine TNF-α and murine IL-2 with the cytomegalovirus (CMV) promoter (Ad-mTNFa and Ad-mIL2, respectively) were constructed as described previously (16, 44).

Killing assay using xCELLigence real-time cell analyzer (RTCA) and in vitro coculture assay. Kinetic analysis of tumor cell lysis was performed using an xCELLigence real-time cell analyzer (ACEA Biosciences) as previously described (49). Ten thousand tumor cells were seeded to the e-plate. After 24-hour culture, tumor cells were infected with 30 virus particles (vp)/cell OAd-TNFa-IL2 or control media. After another 24-hour culture, T cells or control media were added. Cell index was recorded every 20 minutes. For coculture assay, tumor cells were seeded in 48-well plates and infected either with control media or 30 vp/cell of OAd or OAd-TNFa-IL2. After 24 hours, either meso-CAR T cells or control media were added at an effector/target ratio of 1:1. The expression of activation marker CD69 on T cells was analyzed at 72 hours. Total T cell number was determined at day 5 by FCM using CountBright fluorescent beads (Invitrogen).

Study approval. The University of Pennsylvania Institutional Animal Care and Use Committee approved all animal experiments, and all animal procedures were performed in the animal facility at the University of Pennsylvania in accordance with Federal and Institutional Animal Care and Use Committee requirements.

Mouse experiments. NSG and C57BL/6 (B6) (CD45.1 donor and CD45.2 recipient) mice were purchased from Jackson Laboratories. For the human pancreatic tumor xenograft model, NSG mice were subcutaneously injected with 2×10^6 AsPC-1 cells suspended in 100 μl PBS with 50% Matrigel (Corning) into the right flanks. When the mean of tumor volumes reached 200 mm^3, mice were treated with either intratumoral injection of PBS, 0.95×10^9 vp OAd, or 3×10^9 vp OAd-TNFa-IL2 in 50 μl PBS followed by intravenous injection of either PBS, 1×10^6 meso-CAR T cells, or control h19-CAR T cells at day 3 after OAd injection (0.95×10^9 vp of OAd is equivalent to 3×10^9 vp of OAd-TNFa-IL2 in the plaque formation assay).

For the syngeneic mouse PDA tumor-engrafted model, B6 mice were subcutaneously injected with 5×10^5 PDA7940b cells in 100 μl PBS in the right flanks. Established PDA7940b tumors were treated either with intratumoral injection of PBS, 1×10^9 vp of control adenovirus (Ad-luc), or 1:1 mixture of Ad-mTNFa and Ad-mIL2 (total 1×10^9 vp), followed by intravenous injection of either PBS, 5×10^6 mmeso-CAR T cells, or human-CD19-redirected CAR mouse T cells (h19-CAR T cells) at day 1 after Ad injection. Mice were preconditioned with intraperitoneal injection of 120 mg/kg cyclophosphamide at 24 hours before the first T cell injection. Adenovirus and CAR T cell injections were repeated 4 times weekly. Tumor volumes were monitored by caliper measurement.

Tumor and peripheral blood analysis. Tumor dimensions were measured with calipers and the volumes were calculated as follows: volume = (length × $width^2$)/2. Peripheral blood was obtained by retro-orbital bleeding or cardiac puncture and cell numbers of each subset (CD3, CD4, CD8) were quantified using TruCount tubes (BD Biosciences). All experiments were performed in a blind, randomized fashion.

Tumor processing for FCM. AsPC-1 tumors were mechanically diced and then pushed through a 70-μm strainer twice using a syringe plunger and washed with RPMI. PDA7940b tumors were mechanically diced and dissociated by incubating in RPMI media with 100 U/ml collagenase I (Gibco, Life Technologies) and 100 U/ml collagenase IV (Gibco, Life Technologies) at 37°C for 30 minutes. Dissociated cells were passed through a 70-μm cell strainer twice and washed with RPMI media. Cells were then used for FCM analysis.

Tumor homogenate preparation for cytokine assay. Tumor pieces were homogenized with 300 μl ice-cold PBS supplemented with protease inhibitor cocktail (Sigma-Aldrich) in Lysing Matrix D 2-ml tubes (MP Biomedicals) using FastPrep FP120 (Thermo Savant). Tumor homogenate was centrifuged and supernatant was analyzed by high-sensitivity LUMINEX assay per the manufacturer's instructions (Merck Millipore).

IHC and quantification of the staining. IHC was performed on paraformaldehyde-fixed and paraffin-embedded samples. Tumors were cut on a microtome and stained according to the standard protocols. For adenovirus detection, sections were incubated overnight at 4°C with rabbit anti–adenovirus type 2/5 E1A antibody (polyclonal, sc-430, Santa Cruz Biotechnology) at 1:200 dilution, and then incubated with polymer-HRP–conjugated anti-rabbit antibody (DAKO), followed by diaminobenzidine substrate to develop the colorimetric reaction. CD8 was stained with rabbit anti–mouse CD8 Ab (polyclonal, RB-9009-P0, Thermo Fisher Scientific), and mesothelin was stained with mouse anti–human mesothelin Ab (Ab-1, MS-1320-S0, Thermo Fisher Scientific). Stained slides were scanned by ×20 magnification. The number of CD8-positive cells and mesothelin intensity were quantified with Aperio ImageScope software (Leica Biosystems).

T cell trafficking assay. CAR T cell trafficking assays were performed as previously described using CBR-labeled CAR T cells (50). BLI was performed using a Xenogen IVIS-200 Spectrum camera and analyzed with LivingImage software (Caliper Life Sciences).

FCM and antibodies. For FCM analysis, antibodies specific for human CD45 (catalog number, 45-9459-42; clone, 2D1), human FoxP3 (12-4777-42; 236A/E7), and mouse CD3 (11-0032-82; 17A2) were purchased from Affymetrix. Antibodies specific for human CD3 (317322; OKT3), human CD4 (31744; OKT4), human CD69 (310932; FN50), human CD95 (305610; DX2), mouse CD45.1 (110741; A20), mouse CD45.2 (109841; 104), mouse CD3 (100216; 17A2), mouse CD11c (117336; N418), mouse F4/80 (123146; BM8), and mouse CD80 (104712; 16-10A1) were purchased from BioLegend. Antibodies specific for human CD45 (555485; HI30), human CD8 (569179; SK1), human CD25 (335789; 2A3), human Ki67 (561277; B56), mouse CD45 (563410; 30-F11), mouse CD4 (550954; RM4-5), mouse CD8a (563046; 53-6.7), mouse NK-1.1 (560618; PK136), mouse CD11b (550993; M1/70), mouse Ly6C (560595; AL-21), mouse Ly6G (551461; 1A8), and mouse CD86 (560582; GL1) were purchased from BD Biosciences. An antibody specific for human mesothelin (SIG-3623; K1) was purchased from Covance. An antibody specific for mouse mesothelin (LS-C179484; B35) was purchased from LifeSpan BioSciences. Expression of meso-CAR on human T cells was detected with biotinylated goat anti–mouse IgG (specific for scFv of murine origin) (115-065-072; Jackson ImmunoResearch). Expression of mmeso-CAR on mouse T cells was detected with biotinylated goat anti–human IgG

specific for scFv of human origin) (109-116-170; Jackson ImmunoResearch). Cells were stained for viability with violet amine-reactive viability dye (Invitrogen). Surface markers were stained in PBS containing 2% FBS. Intracellular (nuclear) staining was performed using the Foxp3/Transcription Factor Staining Kit (Affymetrix) per the manufacturer's instructions. Mouse tumor and spleen samples were stained after Fc blocking using purified rat anti–mouse CD16/32 antibody (BD Biosciences). All data were collected by a Fortessa LSRII cytometer (BD Biosciences) and analyzed using FlowJo ver. 10 software (Tree Star).

Statistics. Statistical analysis was performed with Prism 5 (GraphPad Software). Two-tailed Student's *t* test was used to compare the 2 groups and 1-way ANOVA with Tukey's post hoc test was used to compare 3 or more groups. Repeated-measures 2-way ANOVA with Bonferroni's correction was used to compare the effect of multiple levels of 2 factors with multiple observations at each level (for tumor volumes, luminescence, and T cell engraftment data). Strength of relationship between 2 factors is presented as Pearson's correlation coefficient. Pearson's *r* values are shown. Survival curves were drawn using the Kaplan–Meier method and the differences of 2 curves were compared with the log-rank test. P values < 0.05 were considered significant.

Author contributions

KW designed experiments, performed experiments, analyzed data, and wrote the manuscript. YL performed experiments and analyzed data. TD performed experiments. SG designed experiments and wrote the manuscript. MR and BK designed experiments. JS designed and performed experiments. RMY designed experiments and coordinated the project. BE provided a critical reagent. SS, MS, RH, and ST performed experiments and provided critical reagents. AH designed experiments, provided a critical reagent, and edited the manuscript. CHJ supervised the project, designed experiments, and wrote the manuscript.

Acknowledgments

This work was supported in part by NIH 5R01CA120409 (to C.H. June), Jane and Aatos Erkko Foundation (to A. Hemminki), HUCH Research Funds (to A. Hemminki), Sigrid Juselius Foundation (to A. Hemminki), Finnish Cancer Organizations (to A. Hemminki), and University of Helsinki (to A. Hemminki). The authors would like to thank Carolyn Shaw, Anna Wing, Shannon E. McGettigan, Andrew Frisch, Pratik Bhojnagarwala, and Susanna Grönberg-Vähä-Koskela for expert technical assistance, Shunnichiro Kuramitsu for helpful discussions on the manuscript and animal sample processing, Gregory Beatty for gift of mouse PDA lines, and Jennifer Brogdon at Novartis Institutes for Biomedical Research.

Address correspondence to: Carl H. June, Smilow Transl. Res. Center, 8-123, 3400 Civic Center Boulevard, Philadelphia, Pennsylvania 19104, USA. Phone: 215.573.3269; Email: cjune@ upenn.edu.

1. Grupp SA, et al. Chimeric antigen receptor-modified T cells for acute lymphoid leukemia. *N Engl J Med*. 2013;368(16):1509–1518.
2. Kochenderfer JN, et al. Chemotherapy-refractory diffuse large B-cell lymphoma and indolent B-cell malignancies can be effectively treated with autologous T cells expressing an anti-CD19 chimeric antigen receptor. *J Clin Oncol*. 2015;33(6):540–549.
3. Locke FL, et al. Phase 1 results of ZUMA-1: A multicenter study of KTE-C19 anti-CD19 CAR T cell therapy in refractory aggressive lymphoma. *Mol Ther*. 2017;25(1):285–295.
4. Beatty GL, O'Hara M. Chimeric antigen receptor-modified T cells for the treatment of solid tumors: Defining the challenges and next steps. *Pharmacol Ther*. 2016;166:30–39.
5. Newick K, Moon E, Albelda SM. Chimeric antigen receptor T-cell therapy for solid tumors. *Mol Ther Oncolytics*. 2016;3:16006.
6. O'Rourke DM, et al. A single dose of peripherally infused EGFRvIII-directed CAR T cells mediates antigen loss and induces adaptive resistance in patients with recurrent glioblastoma. *Sci Transl Med*. 2017;9(399):eaaa0984.
7. Liyanage UK, et al. Prevalence of regulatory T cells is increased in peripheral blood and tumor microenvironment of patients with pancreas or breast adenocarcinoma. *J Immunol*. 2002;169(5):2756–2761.
8. Mukherjee P, et al. MUC1-specific CTLs are non-functional within a pancreatic tumor microenvironment. *Glycoconj J*. 2001;18(11–12):931–942.
9. Moon EK, et al. Multifactorial T-cell hypofunction that is reversible can limit the efficacy of chimeric antigen receptor-transduced human T cells in solid tumors. *Clin Cancer Res*. 2014;20(16):4262–4273.
10. Hassan R, Ho M. Mesothelin targeted cancer immunotherapy. *Eur J Cancer*. 2008;44(1):46–53.
11. Morello A, Sadelain M, Adusumilli PS. Mesothelin-targeted CARs: Driving T cells to solid tumors. *Cancer Discov*. 2016;6(2):133–146.
12. Carpenito C, et al. Control of large, established tumor xenografts with genetically retargeted human T cells containing CD28

and CD137 domains. *Proc Natl Acad Sci USA*. 2009;106(9):3360–3365.
13. Beatty GL, et al. Safety and antitumor activity of chimeric antigen receptor modified T cells in patients with chemotherapy refractory metastatic pancreatic cancer. *J Clin Oncol*. 2015;33(15_suppl):3007.
14. Andtbacka RH, et al. Talimogene laherparepvec improves durable response rate in patients with advanced melanoma. *J Clin Oncol*. 2015;33(25):2780–2788.
15. Lichty BD, Breitbach CJ, Stojdl DF, Bell JC. Going viral with cancer immunotherapy. *Nat Rev Cancer*. 2014;14(8):559–567.
16. Siurala M, et al. Adenoviral delivery of tumor necrosis factor-α and interleukin-2 enables successful adoptive cell therapy of immunosuppressive melanoma. *Mol Ther*. 2016;24(8):1435–1443.
17. Nishio N, et al. Armed oncolytic virus enhances immune functions of chimeric antigen receptor-modified T cells in solid tumors. *Cancer Res*. 2014;74(18):5195–5205.
18. Tanoue K, et al. Armed oncolytic adenovirus-expressing PD-L1 mini-body enhances antitumor effects of chimeric antigen receptor T cells in solid tumors. *Cancer Res*. 2017;77(8):2040–2051.
19. Rosewell Shaw A, et al. Adenovirotherapy delivering cytokine and checkpoint inhibitor augments CAR T cells against metastatic head and neck cancer. *Mol Ther*. 2017;25(11):2440–2451.
20. Kim KH, et al. A phase I clinical trial of Ad5/3-Δ24, a novel serotype-chimeric, infectivity-enhanced, conditionally-replicative adenovirus (CRAd), in patients with recurrent ovarian cancer. *Gynecol Oncol*. 2013;130(3):518–524.
21. Ranki T, et al. Phase I study with ONCOS-102 for the treatment of solid tumors - an evaluation of clinical response and exploratory analyses of immune markers. *J Immunother Cancer*. 2016;4:17.
22. Tähtinen S, et al. Favorable alteration of tumor microenvironment by immunomodulatory cytokines for efficient T-cell therapy in solid tumors. *PLoS One*. 2015;10(6):e0131242.
23. Havunen R, et al. Oncolytic adenoviruses armed with tumor necrosis factor alpha and interleukin-2 enable successful adoptive cell therapy. *Mol Ther Oncolytics*. 2017;4:77–86.
24. Talmadge JE. Immune cell infiltration of primary and metastatic lesions: mechanisms and clinical impact. *Semin Cancer Biol*. 2011;21(2):131–138.
25. Stromnes IM, et al. T cells engineered against a native antigen can surmount immunologic and physical barriers to treat pancreatic ductal adenocarcinoma. *Cancer Cell*. 2015;28(5):638–652.
26. Shultz LD, Ishikawa F, Greiner DL. Humanized mice in translational biomedical research. *Nat Rev Immunol*. 2007;7(2):118–130.
27. Hingorani SR, et al. Trp53R172H and KrasG12D cooperate to promote chromosomal instability and widely metastatic pancreatic ductal adenocarcinoma in mice. *Cancer Cell*. 2005;7(5):469–483.
28. Mantovani A, Marchesi F, Malesci A, Laghi L, Allavena P. Tumour-associated macrophages as treatment targets in oncology. *Nat Rev Clin Oncol*. 2017;14(7):399–416.
29. Nagarsheth N, Wicha MS, Zou W. Chemokines in the cancer microenvironment and their relevance in cancer immunotherapy. *Nat Rev Immunol*. 2017;17(9):559–572.
30. Nakasone Y, et al. Host-derived MCP-1 and MIP-1α regulate protective anti-tumor immunity to localized and metastatic B16 melanoma. *Am J Pathol*. 2012;180(1):365–374.
31. Narumi S, et al. TNF-alpha is a potent inducer for IFN-inducible protein-10 in hepatocytes and unaffected by GM-CSF in vivo, in contrast to IL-1beta and IFN-gamma. *Cytokine*. 2000;12(7):1007–1016.
32. Wolf G, et al. TNF alpha induces expression of the chemoattractant cytokine RANTES in cultured mouse mesangial cells. *Kidney Int*. 1993;44(4):795–804.
33. Wachsmann MB, Pop LM, Vitetta ES. Pancreatic ductal adenocarcinoma: a review of immunologic aspects. *J Investig Med*. 2012;60(4):643–663.
34. Balachandran VP, et al. Identification of unique neoantigen qualities in long-term survivors of pancreatic cancer. *Nature*. 2017;551(7681):512–516.
35. Huh JW, Lee JH, Kim HR. Prognostic significance of tumor-infiltrating lymphocytes for patients with colorectal cancer. *Arch Surg*. 2012;147(4):366–372.
36. Zeng DQ, et al. Prognostic and predictive value of tumor-infiltrating lymphocytes for clinical therapeutic research in patients with non-small cell lung cancer. *Oncotarget*. 2016;7(12):13765–13781.
37. James FR, et al. Association between tumour infiltrating lymphocytes, histotype and clinical outcome in epithelial ovarian cancer. *BMC Cancer*. 2017;17(1):657.
38. Li J, Wang J, Chen R, Bai Y, Lu X. The prognostic value of tumor-infiltrating T lymphocytes in ovarian cancer. *Oncotarget*. 2017;8(9):15621–15631.
39. Son DS, Kabir SM, Dong Y, Lee E, Adunyah SE. Characteristics of chemokine signatures elicited by EGF and TNF in ovarian cancer cells. *J Inflamm (Lond)*. 2013;10(1):25.
40. Robbins RA, Klassen L, Rasmussen J, Clayton ME, Russ WD. Interleukin-2-induced chemotaxis of human T-lymphocytes. *J Lab Clin Med*. 1986;108(4):340–345.
41. Wang H, et al. Desmoglein 2 is a receptor for adenovirus serotypes 3, 7, 11 and 14. *Nat Med*. 2011;17(1):96–104.
42. Siurala M, et al. Adenoviral delivery of tumor necrosis factor-α and interleukin-2 enables successful adoptive cell therapy of immunosuppressive melanoma. *Mol Ther*. 2016;24(8):1435–1443.
43. Ryan DP, Hong TS, Bardeesy N. Pancreatic adenocarcinoma. *N Engl J Med*. 2014;371(11):1039–1049.
44. Tähtinen S, et al. Adenovirus improves the efficacy of adoptive T-cell therapy by recruiting immune cells to and promoting their activity at the tumor. *Cancer Immunol Res*. 2015;3(8):915–925.
45. Brown MC, et al. Cancer immunotherapy with recombinant poliovirus induces IFN-dominant activation of dendritic cells and tumor antigen-specific CTLs. *Sci Transl Med*. 2017;9(408):eaan4220.
46. Yin J, Markert JM, Leavenworth JW. Modulation of the intratumoral immune landscape by oncolytic herpes simplex virus virotherapy. *Front Oncol*. 2017;7:136.
47. Hoogenboom HR, de Bruïne AP, Hufton SE, Hoet RM, Arends JW, Roovers RC. Antibody phage display technology and its applications. *Immunotechnology*. 1998;4(1):1–20.
48. Kanerva A, et al. Enhanced therapeutic efficacy for ovarian cancer with a serotype 3 receptor-targeted oncolytic adenovirus. *Mol*

Ther. 2003;8(3):449–458.
49. Kho D, et al. Application of xCELLigence RTCA biosensor technology for revealing the profile and window of drug responsiveness in real time. *Biosensors (Basel)*. 2015;5(2):199–222.
50. Barrett DM, Liu X, Jiang S, June CH, Grupp SA, Zhao Y. Regimen-specific effects of RNA-modified chimeric antigen receptor T cells in mice with advanced leukemia. *Hum Gene Ther*. 2013;24(8):717–727.